Energy states and magnetization in nanoscale quantum rings

O. Voskoboynikov,[1] Yiming Li,[1,2] Hsiao-Mei Lu,[3] Cheng-Feng Shih,[1] and C. P. Lee[1]
[1]*Department of Electronics Engineering, National Chiao Tung University, Hsinchu 300, Taiwan*
[2]*National Nano Device Laboratories, Hsinchu 300, Taiwan*
[3]*National Tsing Hua University, Hsinchu 300, Taiwan*
(Received 14 April 2002; published 3 October 2002)

In this paper we calculate electron energy states and magnetization for torus shaped nanoscale quantum rings with external magnetic fields. We use the three-dimensional effective one-band Hamiltonian, the energy and position-dependent quasiparticle effective mass approximation, and the Ben Daniel-Duke boundary conditions. The dependence of the energy spectrum on the sizes and shapes of the quantum rings was calculated and the result agrees with experimental observations. Penetration of the magnetic field into torus region results in an aperiodic oscillation of magnetization at zero temperature. It saturates with the increasing of the magnetic field strength.

DOI: 10.1103/PhysRevB.66.155306 PACS number(s): 73.21.−b

I. INTRODUCTION

Microscale and mesoscale metallic and semiconductor quantum rings have been received a considerable attention for decades.[1,2] Advances in the fabrication of semiconductor nanostructures have allowed us to construct nanoscale systems with a wide range of geometries. Recent experimental results on InGaAs torus shaped quantum nanorings demonstrated such capabilities (the typical lateral sizes and height are about 100 nm and 2 nm, respectively.[3–8]) The realization of such semiconductor nanorings bridges the gap between quantum dots and mesoscale ring structures. Unusual excitation properties[4–12] and the capability of trapping a single magnetic flux in such nonsimply connected quantum systems make them attractive for potential practical applications.

The quantum mechanical properties of ring structures have long fascinated physicists. Most of theoretical studies however, either use the traditional one-dimensional (1D) model or assume that the electrons move in a two-dimensional (2D) plane confined by a parabolic potential (see, for instance[5,6,10,13–16] and references therein). Only recently, three-dimensional simulations are performed for torus shaped rings with rectangular[17,18] and cut circle cross sections.[12] These calculations provide explanations for experimental observations in the far-infrared region. It shows an importance of the full 3D description of the nanoscale quantum rings.

To the best of our knowledge, theoretical investigations of the electronic magnetization for 3D nanoscale quantum rings have never been done. It goes without saying that the 3D simulations can obviously provide us with much better understanding of the magnetic quantum phenomena in the nanoscale quantum rings which are expected to be rather different from those in mesoscale rings.

In this paper, we theoretically investigate electron energy systems and magnetization for 3D nanoscale quantum rings. The calculations are done for realistic 3D models of InAs/GaAs quantum rings with the finite hard-wall confinement potential. We use the effective 3D one band Hamiltonian, the energy-dependent (nonparabolic approximation) and position-dependent quasiparticle effective-mass approximation, and the Ben Daniel-Duke boundary conditions. One of the important goals is to go beyond the 1D and 2D parabolic confinement potential pictures. In the 1D approach, varying magnetic field strength B only changes the phase of the electronic wave function, resulting in periodic oscillations in magnetization (the Aharonov-Bohm effect). In the 2D confinement parabolic potential approach the effects of the ring's finite width and the finite hard-wall confinement potential are not considered. In a realistic 3D description, penetration of the magnetic field into the torus region can result in an aperiodic and saturated oscillations in magnetization. Because the main purpose of this paper is to study the effect of ring sizes and geometry on electronic magnetization, we concentrate on a noninteracting electron model at zero temperature. It is known that electron-electron interaction can change electron energy spectrum and the magnetization of nanoscale semiconductor objects.[10] While for single electron quantum ring we present a correct results, calculations of the magnetization of few electron rings are done for reference purposes.

II. THREE-DIMENSIONAL MODEL OF SEMICONDUCTOR QUANTUM RINGS

We assume that quantum rings are formed with the hard-wall confinement potential that is induced by a discontinuity of conduction-band edge of the system components. This model is commonly used to calculate electron energy states in quantum heterostructures[19] and allows us to solve the 3D Schrödinger equation with a minor number of additional approximations. The effective one-band electron Hamiltonian is given in the form

$$\hat{H}=\mathbf{\Pi}_{\mathbf{r}}\frac{1}{2m(E,\mathbf{r})}\mathbf{\Pi}_{\mathbf{r}}+V(\mathbf{r})+\mu_B\frac{g(E,\mathbf{r})}{2}\sigma\mathbf{B}, \qquad (1)$$

where $\mathbf{\Pi}_{\mathbf{r}}=-i\hbar\nabla_{\mathbf{r}}+e\mathbf{A}(\mathbf{r})$ stands for the electron momentum operator, $\nabla_{\mathbf{r}}$ is the spatial gradient, $\mathbf{A}(\mathbf{r})$ is the vector potential ($\mathbf{B}=curl\mathbf{A}$), $m(E,\mathbf{r})$ is the energy and position-dependent electron effective-mass defined by

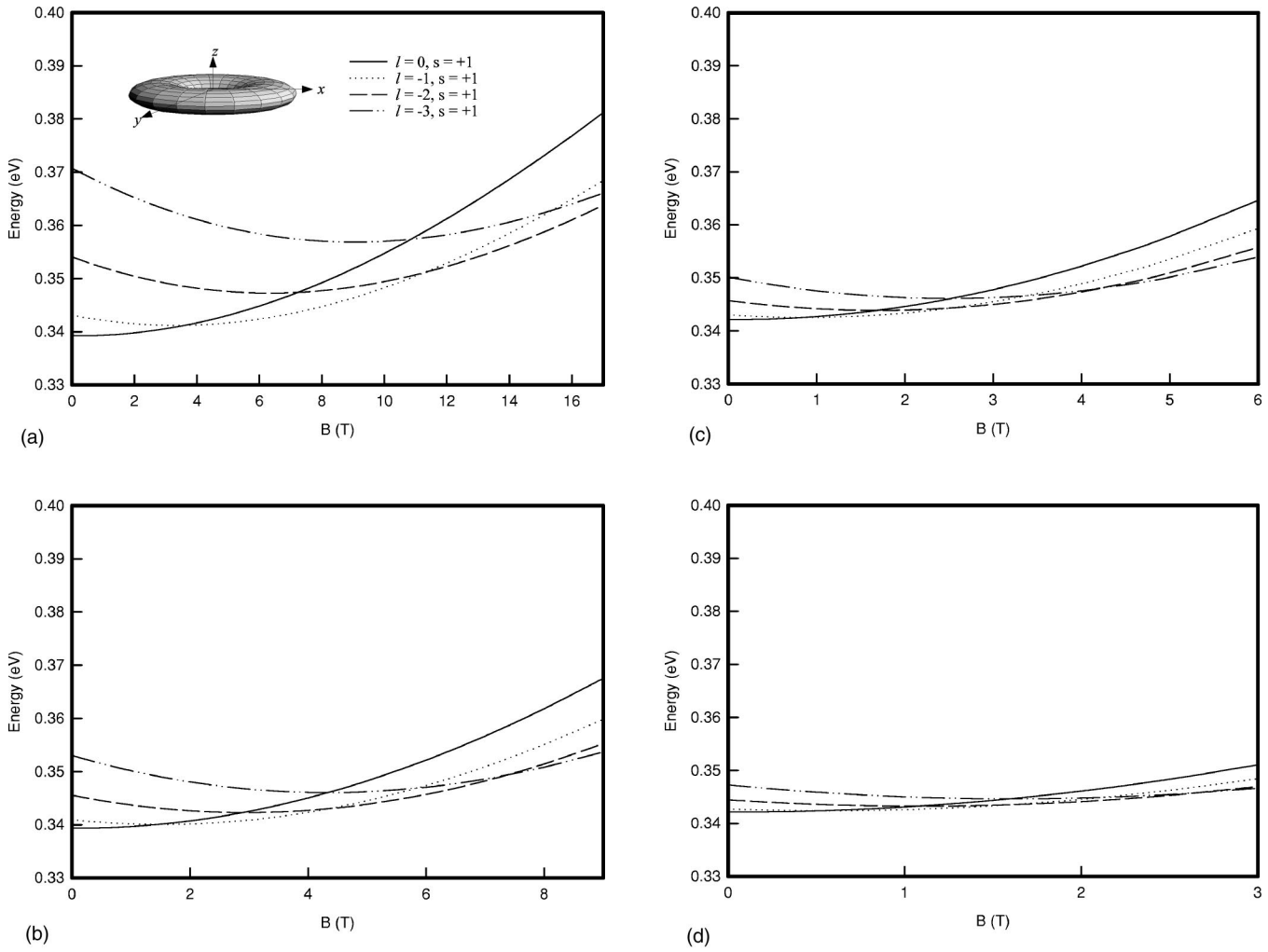

FIG. 1. Electron energy states for TS-InAs nanorings with various inner radii (a) $\rho_{in}=8$ nm, (b) $\rho_{in}=18$ nm, (c) $\rho_{in}=28$ nm, and (d) $\rho_{in}=38$ nm, respectively.

$$\frac{1}{m(E,\mathbf{r})}=\frac{2P^2}{3\hbar^2}\left[\frac{2}{E+E_g(\mathbf{r})-V(\mathbf{r})}+\frac{1}{E+E_g(\mathbf{r})-V(\mathbf{r})+\Delta(\mathbf{r})}\right], \tag{2}$$

and

$$g(E,\mathbf{r})=2\left\{1-\frac{m_0}{m(E,\mathbf{r})}\,\frac{\Delta(\mathbf{r})}{3[E+E_g(\mathbf{r})-V(\mathbf{r})]+2\Delta(\mathbf{r})}\right\} \tag{3}$$

is the Landé factor. In the equations above: $V(\mathbf{r})$ is the confinement potential, $E_g(\mathbf{r})$ and $\Delta(\mathbf{r})$ stand for position-dependent energy-band gap and spin-orbit splitting in the valence band, P is the momentum matrix element, σ is the vector of the Pauli matrices, m_0 and e are the free electron mass and charge. For systems with sharp discontinuity of the conduction-band edge between the inner region of the ring (material 1) and environmental crystal matrix (material 2) the hard-wall confinement potential can be presented as

$$V(\mathbf{r})=\begin{cases}0, & \mathbf{r}\in\mathbf{1}\\ V_0, & \mathbf{r}\in\mathbf{2}.\end{cases}$$

We consider a cylindrically symmetrical quantum ring, which is generated by rotation of a generating contour about z axis. When the magnetic field is directed along the z axis we can treat the problem in cylindrical coordinates (ρ,ϕ,z). The origin of the system is lying in the center of the ring. The generating contours used in the calculation are: an ellipse for torus shaped (TS) rings [see, insert in Fig. 1(a)] and a cut ellipse for cut torus shaped (CTS) ''volcano-type'' rings [see, insert in Fig. 2(a)].[12,20]

Because of the cylindrical symmetry, the wave function can be represented as

$$\Psi(\mathbf{r})=\mathcal{F}(\rho,z)\exp(il\phi),$$

where $l=0,\pm1,\pm2,\cdots$, is the orbital quantum number. This leads to a 2D problem in the (ρ,z) coordinates, and the Schrödinger equation is reduced to

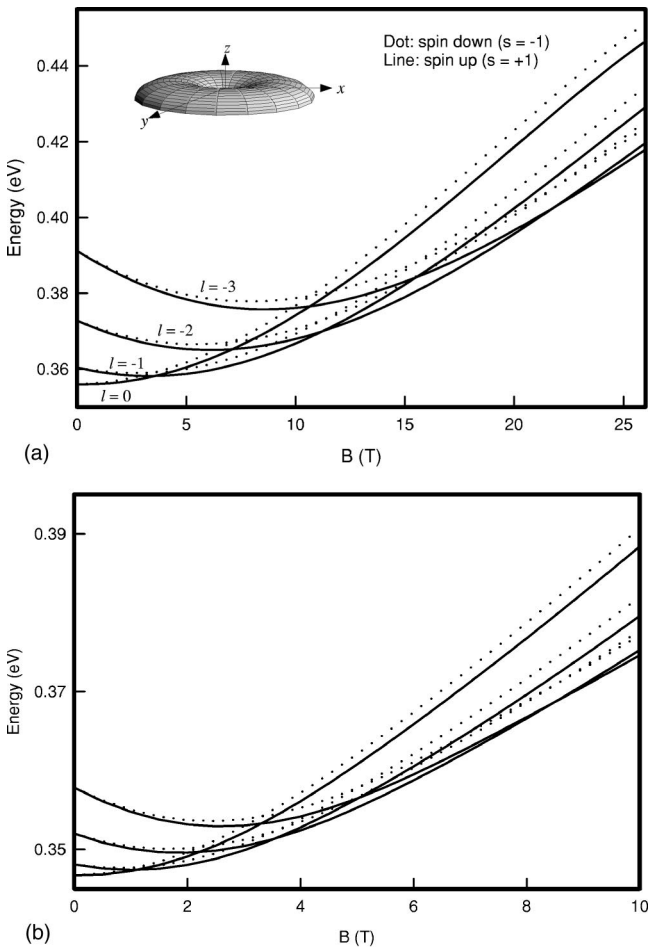

FIG. 2. Electron energy states for CTS-InAs nanorings with outer radius (a) $\rho_{out}=30$ nm and (b) $\rho_{out}=60$ nm.

$$-\frac{\hbar^2}{2m_i(E)}\left(\frac{\partial^2}{\partial z^2}+\frac{\partial^2}{\partial \rho^2}+\frac{1}{\rho}\frac{\partial}{\partial \rho}-\frac{l^2}{\rho^2}\right)\mathcal{F}_l^i(\rho,z)$$
$$+\left[\frac{m_i(E)\Omega_i^2(E)\rho^2}{8}+s\frac{\mu_B}{2}g_i(E)B+\frac{\hbar\Omega_i(E)}{2}l\right.$$
$$\left.+V_0\delta_{i2}-E\right]\mathcal{F}_l^i(\rho,z)=0; \quad i=1,2, \tag{4}$$

where

$$\Omega_i(E)=\frac{eB}{m_i(E)},$$

and $s=\pm 1$ refers to the orientation of the electron-spin along z axis. The Ben Daniel-Duke boundary conditions[19] can be written as the following:

$$\mathcal{F}_l^1(\rho,z)=\mathcal{F}_l^2(\rho,z), \quad z=f(\rho);$$

$$\frac{1}{m_1(E)}\left[\frac{\partial \mathcal{F}_l^1(\rho,z)}{\partial \rho}+\frac{df(\rho)}{d\rho}\frac{\partial \mathcal{F}_l^1(\rho,z)}{\partial z}\right]\Bigg|_{z=f(\rho)}$$
$$=\frac{1}{m_2(E)}\left[\frac{\partial \mathcal{F}_l^2(\rho,z)}{\partial \rho}+\frac{df(\rho)}{d\rho}\frac{\partial \mathcal{F}_l^2(\rho,z)}{\partial z}\right]\Bigg|_{z=f(\rho)}, \tag{5}$$

where $z=f(\rho)$ presents the generating contour of the ring on $\{\rho,z\}$ plane.

The energy states and wave functions of the electrons confined in the quantum ring are found by the nonlinear iterative method. The solution scheme is described somewhere else.[20,21]

III. CALCULATION RESULTS

The quantum rings used in the calculation consist of InAs/GaAs heterostructure. For InAs inside the rings we chose: $E_{1g}=0.42$ eV, $\Delta_1=0.38$ eV, and $m_1(0)=0.024m_0$. For GaAs outside the rings: $E_{2g}=1.52$ eV, $\Delta_2=0.34$ eV, $m_2(V_0)=0.067\ m_0$, and $V_0=0.77$ eV.[22] The energy eigenvalues of the problem (4)–(5) are numerated by a set of quantum numbers $\{n,l,s\}$, where $n=0, 1, 2, \ldots$ is the main quantum number. In Fig. 1 we show the electron energy spectrum versus magnetic fields for TS quantum rings with different inner radii ρ_{in}. The height $h=2.4$ nm and width $\Delta\rho=\rho_{out}-\rho_{in}=24$ nm (ρ_{out} is the outer radius) of the rings are fixed. Only $E_{0,l,+1}(B)$ states are shown for the reason of clarity. It should be mentioned, that for the geometries chosen, the energy difference between two sets $\{0,l,s\}$ and $\{1,l,s\}$ of energy states is controlled by the ring cross-section area and is about the same for all chosen inner radii: $\Delta E=E_{1,0,s}-E_{0,0,s}\simeq 0.298$ eV. However, as it can be seen in Fig. 1, the difference between states of the same n and different l are strongly dependent on the total lateral size of the rings.

In Fig. 2, we present the lowest energy states for two CTS rings of the same height $h=2.4$ nm, inner radius $\rho_{in}=10$ nm, and different outer radii. It should be noted that for bulk InAs (unlike for GaAs) the Landé factor is rather large in absolute value and negative $[g_1(0)\approx -15]$ and, therefore, the Zeeman spin-splitting should be taken into consideration. Unfortunately, the Landé factor behavior in nanoscale semiconductor system has not been well investigated yet and there is a discrepancy in experimental data (see, for instance Refs. 23–26 and references therein). In our calculation the Zeeman spin-spliting is controlled by an average magnitude of the Landé factor $\langle g(E)\rangle$ defined as

$$\langle g(E)\rangle=2\pi\int g(E;\rho,z)|\mathcal{F}_l(\rho,z)|^2\rho d\rho dz.$$

Energy of the lowest states are close for the geometries and sizes chosen (see Fig. 1 and Fig. 2) and the Landé factor depends only weakly of the ring parameters. Our calculation suggests that for instance for the system in Fig. 2(b) $\langle g(E_{0,0,+1};B=0)\rangle=-3.94$ which is close to results calculated in Ref. 27 for small InAs quantum dots. This leads to a small Zeeman spin spliting (even for relatively large magnetic fields it is about a few meV, see, Fig. 2.) which is of no

TABLE I. The $\tilde{k}$ parameter for CTS InAs nanorings.

Ring	First crossing	Second crossing	Third crossing
$\rho_{out}=30$ nm	2.6	7.5	15.2
$\rho_{out}=60$ nm	2.3	7.1	14.5
1D	1	3	5

significance for the following description. In addition, the diamagnetic shift of the energy states for, relatively, weak magnetic fields one can estimate to be proportional to $\langle\rho_l^2\rangle B^2$,[28–30] where

$$\langle\rho_l^2\rangle = 2\pi\int \rho^2|\mathcal{F}_l(\rho,z)|^2\rho d\rho dz.$$

This causes the widening of the energy-band width with respect to the magnetic field: the wider is the ring the wider is the band width both for TS and CTS (see, Fig. 1 and Fig. 2).

We stress that the calculated energy difference ΔE is 21.9 meV for CTS with $\rho_{out}=60$ nm. That is very close to the experimental data[6] and results of other authors calculations.[12] It is worth to be noted, that in contrast to Ref. 12 we do not need to adjust the material band parameters. The averaged effective mass at the lowest level in CTS with $\rho_{out}=60$ nm is estimated to be $m_1(E_{0,0,+1};B=0)=0.042m_0$, which is close to the parameter chosen in Ref. 12.

It is well known that for the quasi-one-dimensional spinless model the single electron ground-state energy of a quantum ring of radius R_0 is given by

$$E_l = E_{\min} + \frac{\hbar^2\left(l+\dfrac{\Phi}{\Phi_0}\right)^2}{2m_1(0)R_0^2}, \tag{6}$$

where $\Phi=\pi R_0^2 B$ is the magnetic flux in the ring and Φ_0 is the flux quanta. With increasing magnetic field, the ground-state changes from a state with $l=0$ to states with $l=-1$, -2, -3, ... and the energy demonstrates a periodic oscillations.[1,2] Crossings between states occur at $\Phi^{\rm cross}/\Phi_0 = k/2$, where $k=1, 3, 5, \ldots$ and the ground state energy minima occur at $\Phi^{\min}/\Phi_0=p$, where $p=0, 1, 2, 3, \ldots$. This Aharonov-Bohm effect[1,2] is a phenomenon inherent to one-dimensional quantum rings.

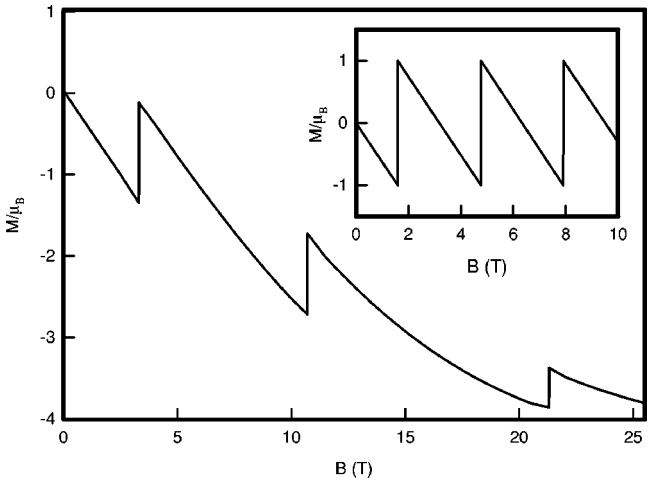

FIG. 3. Magnetization of a single electron CTS-InAs nanoring with $\rho_{out}=30$ nm. The insert is the magnetization for a 1D ring with $R_0=20$ nm.

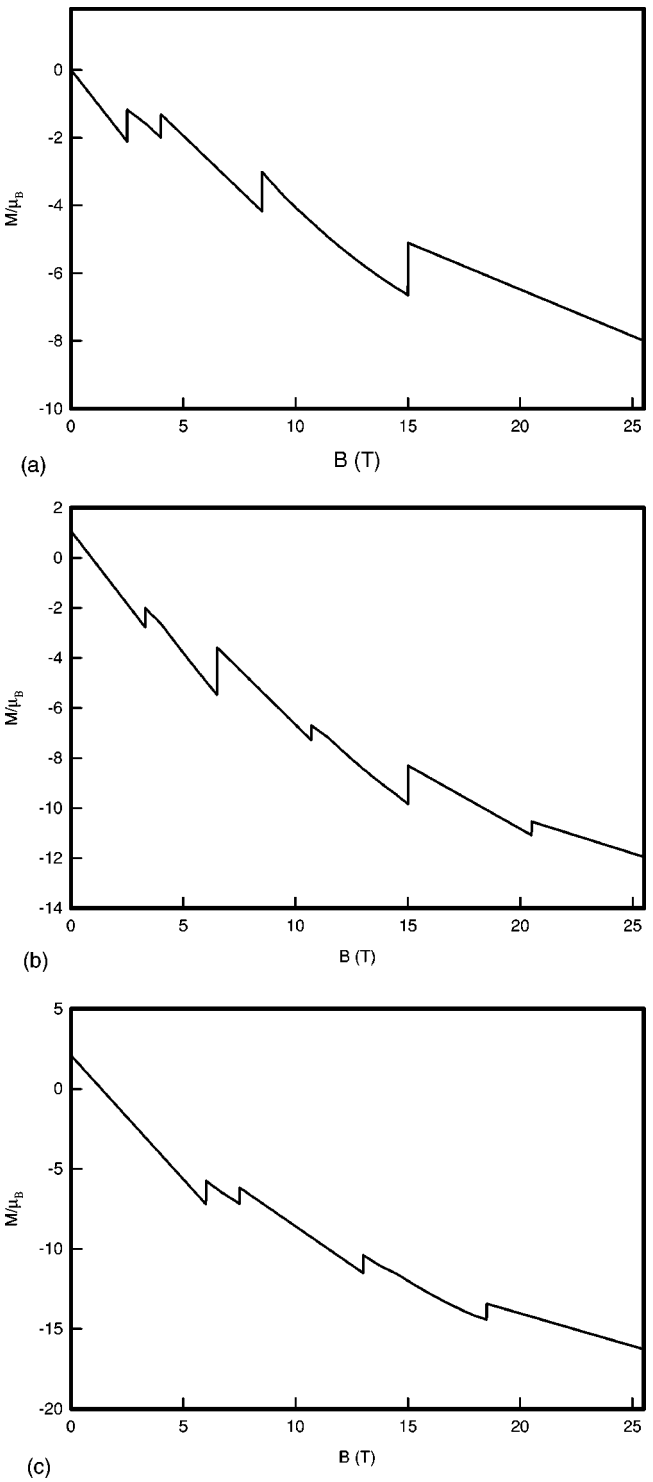

FIG. 4. Magnetizations of CTS-InAs nanorings with a few non-interacting electrons ($\rho_{out}=30$ nm): (a) two, (b) three, and (c) four electrons.

For the 3D nanoscale rings, Fig. 1 and Fig. 2 show a different behavior of the electron ground state. Taking an estimation $\Phi_l = \pi\langle\rho_l^2\rangle B$ one can evaluate $\tilde{k} = 2\Phi_l/\Phi_0$ when the crossing points between states and the ground-state energy minima occur. In Table I, we present results of our calculation for few crossing points in 3D CTS quantum rings. We also found that the lowest point in energy occurs only at $\Phi_0/\Phi_0 = 0$ (only with $p = 0$). The Zeeman spin-spliting leads to small shifts for the crossing points (see Fig. 2). Obviously the oscillatory behavior is not periodic. This difference from the simple rule (6) conforms with experiment[5,6] and demonstrates the importance of a correct three-dimensional description of nanoscale quantum rings.

The aperiodic oscillations have been calculated recently[5,13–15] also in 2D models of the rings. We should notice, that 2D approach allows to study merely the ''lateral spectrum'' of the rings.[16,20] Parameters of the 2D confinement potential and crossing points of the energy states are subjects of a fitting procedure[5,8,13] and one cannot control effects of inner radius and real lateral width of the rings. In contrast, 3D simulations provide us with the adequate choice for quantitative modeling of the electron energy states in nanorings.

Our calculation approach allows us to investigate the magnetization of nanorings. The total magnetization at zero temperature is defined by

$$M = -\frac{\partial E_{tot}}{\partial B}, \tag{7}$$

where

$$E_{tot} = \sum_{n,l,s}^{N} E_{n,l,s}$$

is the total energy for a given N electron system.

It is well known that the magnetization depends drastically on the electron number N. The single-particle picture is yet powerful for magnetic properties of large two-dimensional rings.[15] In Fig. 3 we plot calculated M in units of the effective Born magneton $\mu_B^* = eB/m_1$ as a function of B for single electron CTS ring. The magnetization is an aperiodic and negative function of B and is very different from that obtained by the 1D model (6) (see, insert in Fig. 3). The curve jumps at crossing points of the single electron states. With the increase of the magnetic field the magnetization oscillations become smaller and the magnetization eventually saturates for at large magnetic fields.

For small rings with a few electrons a self-consistent calculation is desirable.[13] Nevertheless, in this work for reference we perform a simulation of the magnetization of quantum rings with a few noninteracting electrons. The simulation results are presented in Fig. 4. The magnetization demonstrates the shell filling sequence. The cylindrical symmetry leads to a complete filling of shells at $N = 2, 6, 12, \ldots$ and the magnetization of such systems is zero at $B = 0$. At the same time, half filled shells provide with a large positive magnetization at $B = 0$.

IV. CONCLUSIONS

In this paper, we calculated energy states and magnetization for nanoscale semiconductor rings. A 3D model of the torus shaped and cut torus shaped rings with various sizes in external magnetic field has been solved numerically.

The calculated dependence of the energy spectrum on ring sizes and shapes agrees with experimental results. At zero temperature, magnetization of the rings oscillate aperiodically as the magnetic field is increased and saturate at very high fields. This is quite different from the Aharonov-Bohm periodic unsaturated oscillation in mesoscopic rings.

Although the internal electronic structure of quantum rings has been explored by far-infrared absorption and other spectral analysis, no measurements of the magnetizations have been made. Based on our theoretical study presented here such measurement of energy shell structure of the nanoscale rings reveal very interesting.

ACKNOWLEDGMENTS

This work was supported in part by the National Science Council of Taiwan under Contracts Nos. NSC-90-2215-E-009-022 and NSC-90-2112-M-317-001.

[1] A.G. Aronov and Yu.V. Sharvin, Rev. Mod. Phys. **59**, 755 (1987).
[2] A. Fuhrer, S. Lüscher, T. Ihn, T. Heinzel, K. Ensslin, W. Wegscheeider, and M. Bichler, Nature (London) **413**, 822 (2001).
[3] J.M. Garsia, G. Medeiros-Ribeiro, K. Schmidt, T. Ngo, J.L. Feng, A. Lorke, J.P. Kotthaus, and P.M. Petroff, Appl. Phys. Lett. **71**, 2014 (1997).
[4] A. Lorke and R.J. Luyken, Physica B **256-258**, 424 (1998).
[5] A. Lorke, R.J. Luyken, A.O. Govorov, J.P. Kotthaus, J.M. Garcia, and P.M. Petroff, Phys. Rev. Lett. **84**, 2223 (2000).
[6] A. Emperador, M. Pi, M. Barranco, and A. Lorke, Phys. Rev. B **62**, 4573 (2000).
[7] R.J. Warburton, C. Schäflen, D. Hafl, F. Bickel, A. Lorke, K. Karrai, J.M. Garcia, W. Schoenfeld, and P.M. Petroff, Physica. E **9**, 124 (2001).
[8] R. Blossey and A. Lorke, Phys. Rev. E **65**, 021603 (2002).
[9] A. Puente and L. Serra, Phys. Rev. B **63**, 125334 (2001).
[10] A. Emperador, M. Pi, M. Barranco, and E. Lipparini, Phys. Rev. B **64**, 155304 (2001).
[11] A. Emperador, M. Barranco, E. Lipparini, M. Pi, and L. Serra, Phys. Rev. B **59**, 15301 (1999).
[12] J. Planelles, W. Jaskólski, and J.I. Aliaga, Phys. Rev. B **65**, 033306 (2002).
[13] T. Chakraboty and P. Pietiläinen, Phys. Rev. B **50**, 8460 (1994).
[14] V. Halonen, P. Pietiläinen and T. Chakraboty, Europhys. Lett. **33**, 377 (1996).
[15] W.C. Tan and J.C. Inkson, Phys. Rev. B **60**, 5626 (1999).
[16] Z. Barticevic, M. Pacheco, and A. Laté, Phys. Rev. B **62**, 6963 (2000).

[17] A. Bruno-Alfonso and A. Latgé, Phys. Rev. B **61**, 15887 (2000).
[18] S.S. Li and J.B. Xia, J. Appl. Phys. **89**, 3434 (2001).
[19] G. Bastard, *Wave Mechanics Applied to Semiconductor Heterostructures* (Les Edition de Physique, Les Ulis, 1990).
[20] Y. Li, O. Voskoboynikov, C. P. Lee, C.-F. Shih, S. M. Sze, and O. Tretyak, in *Proceedings of the 2001 First IEEE Conference on Nanotechnology, IEEE-NANO, 2001*, edited by C. Lau (IEEE, Maui, Hawaii, 2001), p. 11.
[21] Y. Li, O. Voskoboynikov, C.P. Lee, S.M. Sze, and O. Tretyak, J. Appl. Phys. **90**, 6416 (2001); Y. Li, O. Voskoboynikov, C.P. Lee, and S.M. Sze, Comput. Phys. Commun. **141**, 66 (2001); Solid State Commun. **120**, 79 (2001).
[22] *Handbook Series on Semiconductor Parameters*, edited by M. Levinshtein, S. Rumyantsev, and M. Shur (World Scientific, Singapore, 1999).
[23] A.S.G. Thornton, T. Ihm, P.C. Main, L. Eaves, and M. Henini, Appl. Phys. Lett. **73**, 354 (1998).
[24] M. Bayer, A. Kuther, F. Schäder, J.P. Reithmaier, and A. Forchel, Phys. Rev. B **60**, R8481 (1999).
[25] J.-M. Meyer, I. Hapke-Wurst, U. Zeitler, R.J. Haug, and K. Pierz, Phys. Status Solidi B **224**, 685 (2001).
[26] G. Medeiros-Ribeiro, M.V.B. Pinheiro, V.L. Pimentel, and E. Marega, Appl. Phys. Lett. **80**, 4229 (2002).
[27] A.A. Kiselev, E.L. Ivchenko, and U. Rössler, Phys. Rev. B **58**, 16353 (1998).
[28] J.J. Field and D.G. Thomas, Phys. Rev. **122**, 35 (1961).
[29] A.V. Chaplik, Zh. Exp. Theor. Fiz. **119**, 193 (2001) [JETP **92**, 169 (2001)].
[30] K.L. Janssens, F.M. Peeters, and V.A. Schweigert, Phys. Rev. B **63**, 205311 (2001).